Allosteric control in a metalloprotein dramatically alters function

Elizabeth Leigh Baxter[a,b,1], John A. Zuris[a,1], Charles Wang[a], Phu Luong T. Vo[a], Herbert L. Axelrod[c], Aina E. Cohen[c], Mark L. Paddock[a], Rachel Nechushtai[d], Jose N. Onuchic[b,e], and Patricia A. Jennings[a,2]

[a]Department of Chemistry and Biochemistry and [b]Center for Theoretical Biological Physics, University of California at San Diego, La Jolla, CA 92093; [c]Stanford Synchrotron Radiation Lightsource, Menlo Park, CA 94025; [d]The Alexander Silberman Institute of Life Science, Hebrew University of Jerusalem, Jerusalem 91904, Israel; and [e]Center for Theoretical Biological Physics and Departments of Physics and Astronomy, Chemistry, and Biochemistry and Cell Biology, Rice University, Houston, TX 77050

Edited by William A. Eaton, National Institute of Diabetes and Digestive and Kidney Diseases, National Institutes of Health, Bethesda, MD, and approved November 27, 2012 (received for review May 16, 2012)

Metalloproteins (MPs) comprise one-third of all known protein structures. This diverse set of proteins contain a plethora of unique inorganic moieties capable of performing chemistry that would otherwise be impossible using only the amino acids found in nature. Most of the well-studied MPs are generally viewed as being very rigid in structure, and it is widely thought that the properties of the metal centers are primarily determined by the small fraction of amino acids that make up the local environment. Here we examine both theoretically and experimentally whether distal regions can influence the metal center in the diabetes drug target mitoNEET. We demonstrate that a loop (L2) 20 Å away from the metal center exerts allosteric control over the cluster binding domain and regulates multiple properties of the metal center. Mutagenesis of L2 results in significant shifts in the redox potential of the [2Fe-2S] cluster and orders of magnitude effects on the rate of [2Fe-2S] cluster transfer to an apo-acceptor protein. These surprising effects occur in the absence of any structural changes. An examination of the native basin dynamics of the protein using all-atom simulations shows that twisting in L2 controls scissoring in the cluster binding domain and results in perturbations to one of the cluster-coordinating histidines. These allosteric effects are in agreement with previous folding simulations that predicted L2 could communicate with residues surrounding the metal center. Our findings suggest that long-range dynamical changes in the protein backbone can have a significant effect on the functional properties of MPs.

allostery | CISD1 | energy landscape theory | iron-sulfur cluster | protein frustration

Metalloproteins (MPs) comprise nearly one-third of all known protein structures and are classified by their unique inorganic moieties. Examples are the copper-containing cupredoxins, iron-sulfur proteins, nickel-containing hydrogenases, and numerous others (1–3). The incorporation of metals allows for thousands of new biological catalysts, capable of performing chemistry that would otherwise be impossible using only the amino acids found in nature. The widely held view of MPs is that the properties of the metal centers are primarily dictated by the "inner sphere," which consists of the coordinating ligands and to a lesser extent local residues that can influence both the electrostatic environment, as well as hydrophobic residues that can act like wires and funnel electron density (4). The redox properties of MPs tend to be influenced by only a small fraction of the amino acids in the protein, generally those directly bonded to, or in close proximity to, the metal center (5). Indeed, it has been shown that the local scaffold of a metallic redox center can by chemically synthesized to mimic the active site of the protein, and in many cases, the electron transfer properties of these metalloproteins can be reproduced and better understood in these simplified ligand environments (4).

Iron-sulfur (FeS) cluster-containing proteins make up the largest class of MPs and are major players in human health and disease (6). They play critical roles as electron transfer proteins in processes such as photosynthesis, cellular respiration, nitrogen fixation (7, 8), and catalysis (1). The newest member of the FeS cluster protein family, mitoNEET, is a uniquely folded homodimeric [2Fe-2S] protein, with each monomer bearing a single [2Fe-2S] cluster (9–11) (Fig. 1*A*). The clusters are ligated in a rare 3-Cys-1-His coordination sphere (Fig. 1*B*), where the single His is critical for function (12, 13) and drug binding (14). MitoNEET is a target of the thiazolidinedione (TZD) class of anti–type II diabetes drugs and is the first known FeS protein to be targeted by drug binding (15). We discovered that mitoNEET functions as a cluster transfer protein and can donate its cluster to an apo-acceptor protein and into mitochondria under oxidative stress conditions (13). These stress conditions are commonly found in patients with diabetes (16, 17). TZD binding blocks cluster transfer in vitro and iron overload in vivo, a condition commonly associated with type II diabetes (13). An interesting hypothesis is that abrogation of mitochondrial iron overload by treatment of cells with small molecules such as TZDs is a result of changes in mitoNEET's cluster properties and is an active area of inquiry.

We recently used energy landscape theoretical studies to investigate the factors that govern cluster properties in mitoNEET (18, 19). Briefly, energy landscape theory indicates that proteins fold in a funneled fashion with minimal frustration, with the native state and functional fluctuations occurring toward the bottom of this funnel (20, 21). Because proteins are active on the same landscape that they fold on (22), their functional motions may introduce ruggedness in to the folding landscape. For example, functional loop mutations in WW domain proteins speed up folding at the expense of function and in some cases remove the barrier to folding completely (23, 24). Additionally, energetic frustration in proteins colocalize with cofactor binding sites (25). Simulations with the β trefoil family of proteins demonstrated that strain in a functionally important β bulge was responsible for the slow folding of the family (26–28). Thus, identifying residues that contribute frustration in folding may be an effective way to predict and identify important sites for protein–protein interactions, as well as new binding regions for potential drug targets.

Author contributions: E.L.B. and M.L.P. designed research; E.L.B., J.A.Z., C.W., P.L.T.V., H.L.A., and A.E.C. performed research; E.L.B., J.A.Z., H.L.A., A.E.C., R.N., J.N.O., and P.A.J. analyzed data; and E.L.B., J.A.Z., H.L.A., R.N., J.N.O., and P.A.J. wrote the paper.

The authors declare no conflict of interest.

This article is a PNAS Direct Submission.

Freely available online through the PNAS open access option.

Data deposition: The atomic coordinates and structure factors have been deposited in the Protein Data Bank, www.pdb.org [PDB ID code 4EZF (RCSB072261); PDB ID code 4F28 (RCSB072362); PDB ID code 4F1E (RCSB072332); PDB ID code 4F2C (RCSB072366)].

[1]E.L.B. and J.A.Z. contributed equally to this work.

[2]To whom correspondence should be addressed. E-mail: pajennings@ucsd.edu.

This article contains supporting information online at www.pnas.org/lookup/suppl/doi:10.1073/pnas.1208286110/-/DCSupplemental.

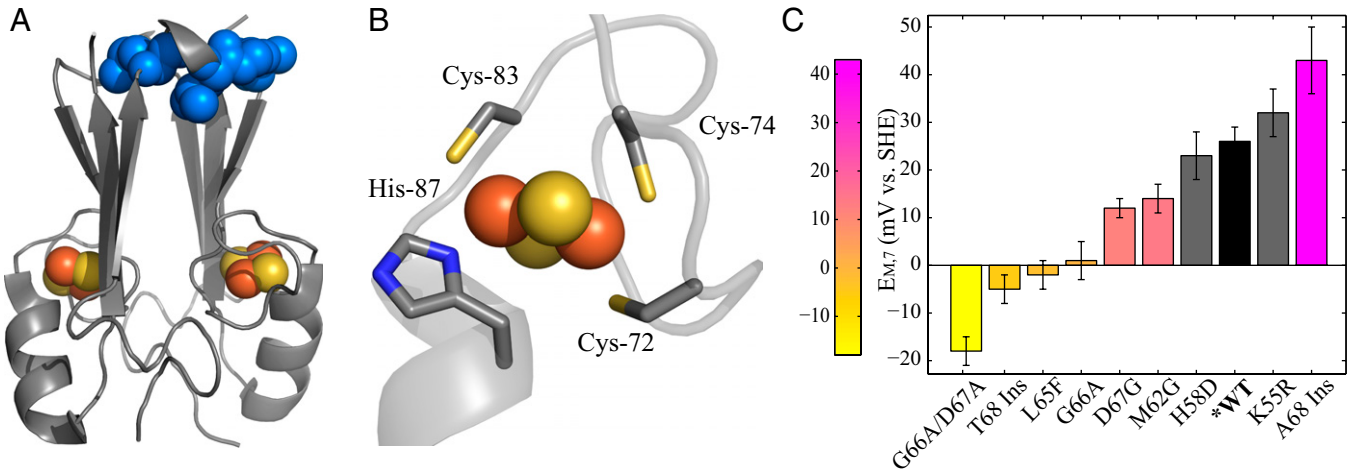

Fig. 1. Mutagenesis of distal residues in L2 result in both positive and negative shifts in the [2Fe-2S] cluster redox potential at pH 7 ($E_{M,7}$). (*A*) Mutated residues in L2 are colored in blue on the structure of mitoNEET. (*B*) The [2Fe-2S] cluster is coordinated by three cysteines and one histidine. (*C*) $E_{M,7}$ values for WT mitoNEET and L2 mutants span a range of ~60 mV. $E_{M,7}$ values are adjusted to standard hydrogen electrode (SHE) values, with errors indicated by cross bars. WT is shown in black, and controls are shown in gray.

Whether energy landscape theory can predict functional control in metalloproteins is an open question. We used this theory together with structure-based models (SBMs) (29–31) to investigate the landscape of mitoNEET and predicted a loop distal to the [2Fe-2S] cluster (L2) that constrains folding and controls the motions of the cluster-binding domain. We hypothesized that, despite being ~20 Å removed from the [2Fe-2S] cluster, this frustrated loop region may function as an allosteric control site, regulating functional properties of the [2Fe-2S] moiety (18). In our current study, we test this hypothesis by experimentally introducing perturbations into this distal loop (Fig. 1*A*) and analyze the properties of the [2Fe-2S] cluster. Point mutations and insertion of new residues in L2 significantly reduce cluster stability and can accelerate mitoNEET cluster transfer to apo-acceptor proteins by a factor of 15-fold. These perturbations in L2 also shift the redox potential by up to ~60 mV, indicating that long-range effects regulate cluster stability, cluster transfer, and electron transfer potential in this system. A common interpretation of these results would be that mutation alters the structure of the protein, especially the cluster-binding region. Strikingly, the crystal structures of the mutant proteins show no changes in overall fold or in the cluster-binding domain. The only difference observed is in a single mutant protein with the necessary elongation of the distal loop on insertion mutagenesis. Taken together with native-basin simulations, we suggest correlated motions between L2 and the protein scaffold provide distal allosteric control of the [2Fe-2S] cluster making L2 an interesting site for targeting with drug design.

Results

Perturbations in the L2 Region Induce Long-Range Changes in the Redox Potential of MitoNEET's [2Fe-2S] Cluster. Mutagenesis of several residues in the L2 region (Fig. 1*A*, blue spheres) led to significant changes in the redox potential ($E_{M,7}$) of the protein's cluster (Fig. 1*C*). We used optical spectroelectrochemical titrations (32) to measure redox potentials of various L2 mutants. We mutated Met62 and Asp67 to Gly to relax L2 and allow greater flexibility in the β cap domain. These M62G and D67G mutants showed $E_{M,7}$ decreases of −12 and −14 mV, respectively, from the WT $E_{M,7}$ value of +26 ± 3 mV (32). Importantly, these shifts are ionic strength independent suggesting that factors other than electrostatics control the redox properties. Therefore, we introduced an aromatic group in the L2 region that would potentially stabilize L2 with increased hydrophobic packing between protomers. We found that this mutation induced an even greater shift in $E_{M,7}$ value, which is 28 mV less than WT. We also found that reducing flexibility of residue 66 by replacing Gly with Ala (G66A) shifted the $E_{M,7}$ ~ −25 mV. The G66A/D67A double mutant was designed to increase the helicity of the L2 region and interestingly led to the largest $E_{M,7}$ shift from the WT protein of ~44 mV (−18 ± 3 mV for G66A/D67A compared with +26 ± 3 mV). Finally, opposite changes in $E_{M,7}$ were induced by the choice of residue inserted at position 68 in the amino acid sequence. Insertion of alanine (A68 insert) led to a positive increase in the $E_{M,7}$ value to +43 ± 7 mV. Alanine is known to be a helix maker, and as a result, we wanted to determine whether the insertion of a helix breaker, such as threonine, would induce similar or opposite changes in the $E_{M,7}$. We found that insertion of threonine (T68 insert) caused a decrease in $E_{M,7}$ to a new value of −5 ± 4 mV, which is 31 mV less than the WT. These long-range redox changes are observed despite the fact that the mutated residues are between 18 and 26 Å away from the [2Fe-2S] cluster, as measured both intraprotomer and interprotomer. To test whether mutagenesis of any region of the protein is capable of resulting in redox changes, we introduced two additional mutations as controls: K55R and H58D. In both cases, the shift in redox potential is <5 mV, despite the fact that these mutations are 7.5 and 9.7 Å away from the [2Fe-2S] cluster, respectively (Fig. 1). Taken together, our results show that residues in the L2 region (Fig. 1*A*, shown in blue) can communicate with the distally located cluster binding region of the protein and change cluster redox properties.

L2 Region Strongly Influences the Cluster Transfer Function of MitoNEET and the Innate Stability of Its [2Fe-2S] Cluster. We discovered that mitoNEET functions as a [2Fe-2S] cluster transfer protein (13). Having shown that allosteric changes in the L2 region are able to affect redox properties (Fig. 1), we hypothesized that L2 may also play an important role in cluster transfer. Both the M62G and L65F show significant increases in cluster transfer (Fig. 2*A*) compared with that observed for the WT protein. The largest shift was seen in the M62G mutant, which transferred over 10-fold faster than the WT (Fig. 2*A*). Conversely, cluster transfer is slowed in the G66A, D67G, and G66A/D67A mutant proteins. Finally, both the A68 and T68 insertion mutations showed very similar transfer rates to one

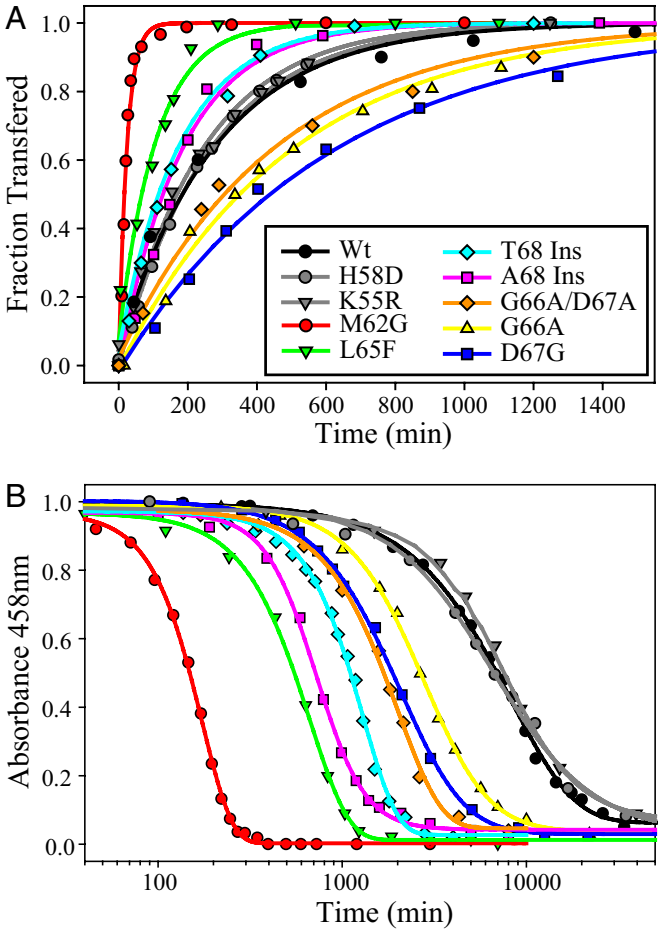

Fig. 2. L2 region strongly influences [2Fe-2S] cluster transfer function of mitoNEET and cluster stability. (*A*) Transfer of the [2Fe-2S] cluster from mitoNEET and L2 mutants to apo-ferredoxin. Cluster transfer experiments were performed aerobically at 37 °C at pH 8.0 using 100 μM mitoNEET or L2 mutants and 100 μM apo-ferredoxin in 50 mM Bis-Tris and 100 mM NaCl. (*B*) Stability of mitoNEET's [2Fe-2S] cluster compared with L2 mutants. Cluster stability measurements were performed aerobically at 37 °C. Loss of the [2Fe-2S] cluster was measured over time as a decrease in absorbance at 458 nm. Studies were performed using 40 μM mitoNEET or L2 mutants in 100 mM Bis-Tris and 100 mM NaCl, pH 7.0. WT is shown in black, and controls are shown in gray.

another (Fig. 2*A*), even though they induce opposite shifts in $E_{M,7}$ (Fig. 1*C*). We conclude that the L2 region is able to dramatically affect protein function through allosteric effects on the distal [2Fe-2S] clusters.

In addition to cluster transfer, the [2Fe-2S] cluster in mitoNEET may be important for binding to other proteins and small molecule effectors. Besides inhibiting cluster transfer, TZDs are known to stabilize mitoNEET's cluster against release (9). As mitoNEET's cluster stability is dramatically affected by drug binding (9), it is also important to examine the effect that L2 mutants have on cluster stability. We assayed our loop mutants for cluster stability by monitoring loss of the mitoNEET's 458-nm absorbance peak over time as described previously. We found that all L2 mutations caused lower stability in the [2Fe-2S] cluster (Fig. 2*B*). However, cluster transfer rates do not correlate with cluster stability, indicating that allosteric effects can influence interactions important for cluster transfer and protein stability, although these two effects are independent of one another. Fig. 2 also includes data for the K55R and the H58D mutations, which show no change in either cluster transfer rates or cluster stability from WT. We summarized our findings on the influence of L2 residues for redox potential, cluster transfer, and cluster stability in Table S1.

Structural Integrity of the Protein Is Maintained on L2 Mutation. To determine whether the L2 mutation effects on cluster properties were the result of conformational rearrangements in the protein, we initiated structural analyses and subsequently obtained crystal structures for the G66A/D67A, A68 insert, M62G, and D67G mutant proteins and compared them to the WT structure (9–11) (Fig. 3) (Table S2). Overall, the entire structural fold remains intact on mutation in L2. In all cases, the cluster-binding domain of the mutant protein is superimposable with that of the WT protein (Fig. 3 *A* and *B*). Only small local changes are observed in the L2 region as a result of the necessary accommodation on insertion of a residue between residues 67 and 68 to make the A68 insertion (Fig. S1). The D67G mutation crystallized with a completely different set of crystal packing interactions, suggesting that the lack of conformational changes is not a result of crystal packing forces. For example, in the D67G structure, a packing interaction exists between Lys68 and Asp64; however, this packing interaction is not observed in the WT structure. Therefore, mitoNEET is well folded and robust to mutation. We also measured the optical spectrum of the L2 mutants to probe for possible cluster binding changes in the proteins that were not crystallized. We found that all seven L2 mutants have absorption spectra identical to that observed for WT (Fig. 3*C*). The similarity of the spectra is important as we have found that replacement of the cluster-coordinating His87 ligand led to noticeable changes in the visible region (12, 33) (Fig. S2) and also that mutations that affected the pK_a of His87, namely Lys55, led to small but measureable optical shifts of ~3 nm near the signature 458-nm absorption peak (32). The absence of any spectral shifts taken together with crystallographic analyses indicates that mutations do not alter the overall fold or the cluster binding environment.

All-Atom Simulations Demonstrate Communication Between L2 and the Cluster-Coordinating Histidine. To probe possible mechanisms of cluster property regulation, we investigated the fluctuations of the WT protein in the native basin with SBM simulations. These models are based on energy landscape theory (21) and accurately describe the native state ensemble fluctuations of many systems (31, 34–38). We performed simulations with an all-atom SBM with interactions present in the crystal structure as stabilizing, and with one energetic basin describing the folded state. To examine possible mechanisms whereby distal regions exert control over the [2Fe-2S] cluster, we examined the motions within the native basin and plotted correlated motions in a covariance matrix (Fig. S3). The covariance matrix is overlaid with a contact map of the protein in black squares for clarity. Regions of correlated motions are plotted in red, circled, and mapped onto the protein to designate intra- (Fig. S3 *A* and *C*) and interprotomer (Fig. S3 *B* and *D*) covariance.

The distribution of correlated motions on the protein shows that the L2 region is motionally coupled to regions on the opposite end of the protein. Aside from residues that are in direct contact with each other, regions toward the center of the protein show little correlated motion. To further characterize these motions, we use principle component analysis to extract the large-scale collective motions from the trajectory. The collective motions of the Cα atoms for the first eigenvector are plotted in Fig. 4 with 10 superimposed frames from a movie of the first eigenvector. The initial starting frame is colored white, with each subsequent frame moving from white to red for protomer A and white to blue for protomer B. From the top view, the protein exhibits a torsional motion with $L2_A$ and $L2_B$ twisting together at the top of the β cap domain in the foreground and the cluster-binding domain moving in the opposite direction in the background (Fig. 4*A*). The side view of the protein (Fig. 4*B*) shows that the twisting of the β cap domain results in scissoring in the

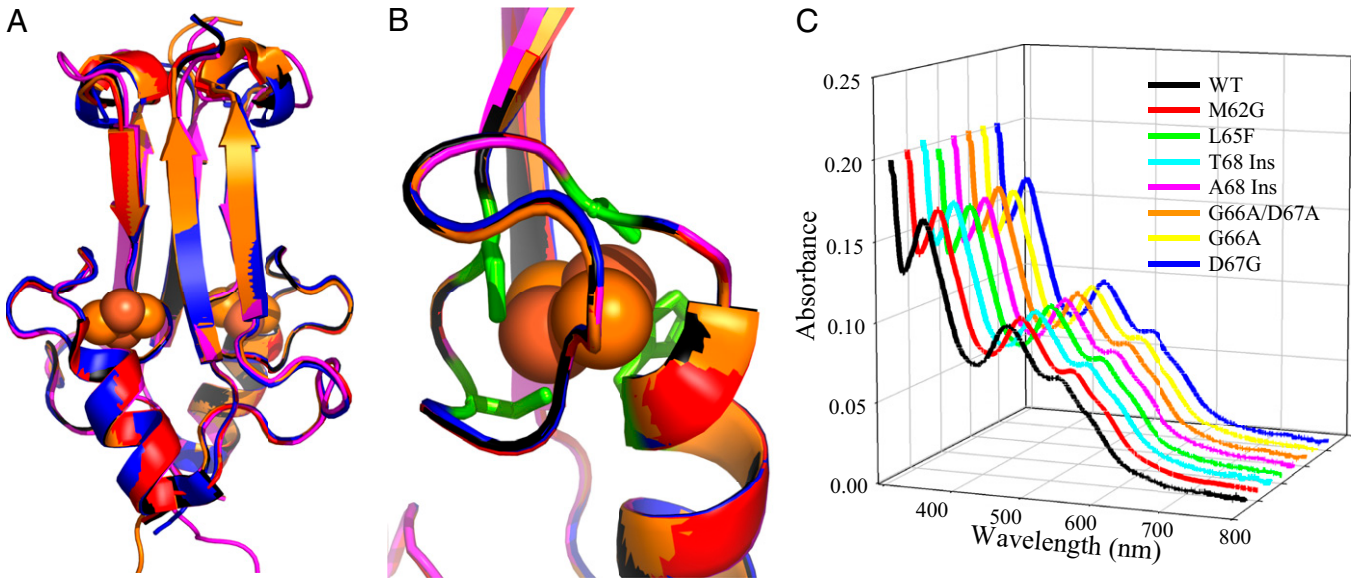

Fig. 3. Structural analysis of L2 mutants show no conformational changes. (*A*) Crystal structures of the G66A/D67A (PDB ID code 4F2C), A68 insert (PDB ID code 4EZF), M62G (PDB ID code 4F28), and D67G (PDB ID code 4F1E) mutants are overlaid with WT mitoNEET. (*B*) An overlay of the cluster binding domains and the cluster coordinating ligands show that the cluster coordinating pockets of all L2 mutants are superimposable with that of WT mitoNEET. (*C*) The UV-visible spectra of all seven L2 mutants are identical to that observed for WT. The absorption spectra reports on the environment near the [2Fe-2S] cluster.

cluster binding domain, where $\alpha1_A$ and $L1_B$ move together opposite of $\alpha1_B$ and $L1_A$. Interestingly, the [2Fe-2S] clusters appear to be a pivot point for these motions, so that the entire protein rearranges around the cluster-binding region. Much of the cluster-coordinating pocket, including the coordinating cysteines, exhibit little motion relative to the rest of the protein; however, the Cα atom for the coordinating histidine exhibits a much larger range of motion (Fig. 4*C*). Because the coordinating histidine is positioned at the bottom of α1, it scissors with α1 away from the cluster-coordinating pocket in response to twisting in L2.

Discussion

In conventional systems, the properties of metalloproteins are controlled by local ligand environment. Complex biological systems include an additional control involving the use of strain to exert long-range coupling (27, 39). A simple analogy for this type of control is a clothes pin, where a strained spring is necessary for regulating clasp and release. Pinching a clothes pin at one end rearranges everything around a central pivot point and induces the largest motions at the opposite end of the structure. In

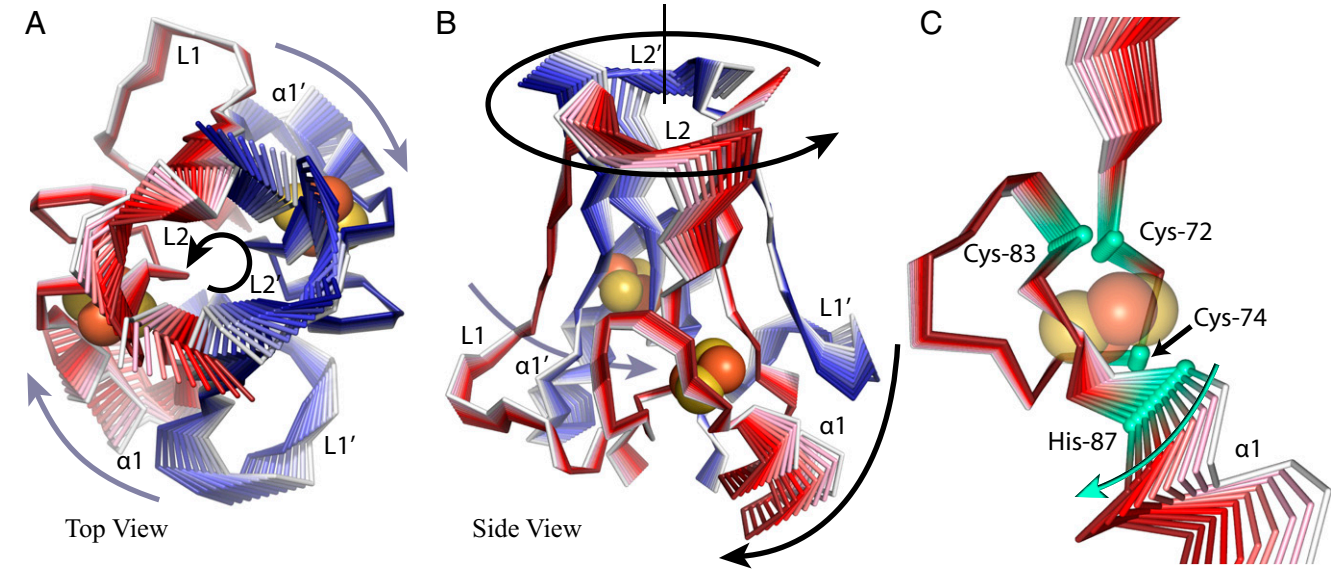

Fig. 4. Twisting in L2 controls swinging of His87. (*A*) Ten frames from the collective motions of the Cα atoms for the first eigenvector are superimposed. The initial starting point is colored white, with each subsequent frame moving from white to red for protomer A and white to blue for protomer B. From the top view, the protein exhibits a torsional motion with L2 and L2′ twisting together at the top of the β cap domain in the foreground, and the cluster binding domain moving in the opposite direction in the background. (*B*) The side view of the protein shows that the twisting of the β cap domain results in scissoring of α1 and L1′ with α1′ and L1 in the cluster binding domain, with the [2Fe-2S] cluster acting as a hinge point. (*C*) The backbone of the cluster-coordinating pocket and the coordinating cysteines shows little movement; however, the coordinating histidine swings open in response to twisting in L2.

mitoNEET, twisting or "pinching" of L2 triggers scissoring at the bottom of the cluster binding domain, so that $\alpha1_A$ and $L1_B$ scissor against $\alpha1_B$ and $L1_A$. The [2Fe-2S] cluster is positioned at the pivot point of these motions, and much of the cluster-binding pocket, including the cluster-coordinating cysteines, exhibits little motion. However, twisting of L2 causes the entire protein to rearrange around the metal center and results in the coordinating histidine swinging away from the metal center (Fig. 4). Mutations that alter the flexibility, or expand or collapse L2, may alter the degree to which the coordinating histidine moves. This rearrangement of the protein backbone (Fig. 4 *A* and *B*), especially at the coordinating histidine (Fig. 4*C*), may account for the measured redox shifts and more importantly the order of magnitude increase in the rate of cluster transfer to an apo-acceptor protein (Fig. 1).

A protein undergoing such hinging motions may move through energetically less favorable states. It has been proposed that partially unfolded states may compete energetically with some of these higher energy states, relieving strain (34). This local unfolding, or cracking (34), is important for the activity for many proteins, and indeed there are cases where the addition of denaturant can speed up enzymatic activity (40–42). In mitoNEET, cracking may be an essential part of the cluster transfer mechanism. An apo-acceptor protein could pinch L2, which would result in displacement of residues in α1 and L1 in the cluster binding domain (Fig. 4). This displacement could create strain on the protein, causing it to "crack" open and increase accessibility of the metal center, which may lead to decreased cluster stability or enhanced cluster transfer. However, it is important to note that cluster stability and transfer efficiency are not necessarily linked (13). In the present studies, all L2 mutations increase cluster decay rates. However, not all mutations speed up cluster transfer. Mutations to residues 62, 65, and 68 all increase cluster transfer (Fig. 2*A*); however, mutations to residues 66 and 67 slow down cluster transfer despite being destabilizing, suggesting different mechanisms governing cluster stability vs. transfer. One hypothesis for this is that all mutations increase cracking in L1 and α1 and thus increase decay rate; however, residues 66 and 67 may be important for the binding interaction with apo-acceptor proteins. The largely negative charge on the surface of the β cap may be a docking site for a mitoNEET protein partner, and judging by the major functional effects that perturbation of the L2 region indeed has on its cluster properties, we postulate that this is likely the case.

Conclusions

We used a combination of experimental techniques and structure-based simulations to test the hypothesis that a distal loop in mitoNEET acts as regulatory control region for the [2Fe-2S] cluster (19). Mutagenesis to L2 results in significant destabilization of the [2Fe-2S] cluster and can either abrogate or accelerate cluster transfer by a factor of up to 15-fold. Additionally, these perturbations to L2 20 Å from the 2Fe-2S cluster result in significant shifts in redox potential, thus demonstrating that the L2 region is able to distally regulate functional properties of the protein found in the cluster-binding domain. As the most dramatic mutations do not involve charged amino acids, the observed shifts in redox potential over the 20-Å distance cannot be caused by electrostatic effects. Crystal structures obtained for several mutants show that the cluster-binding domains of the mutant proteins are superimposable with that of the WT protein, indicating that these effects are also not the result of a long-range conformational change. Using structure-based simulations, we propose a mechanism of communication in which twisting in L2 triggers scissoring in the cluster-binding domain and results in displacement of the coordinating histidine. This long-range allosteric control of the metal center suggests that many other MPs may in fact require full use of their uniquely evolved scaffolds to perform complex biological tasks. Taken together, this work provides a foundation for investigating how metal centers in metalloproteins are influenced by the global motions and expands our understanding beyond the control of simple electron transfer by distal mutations (43). This approach is critical for designing new therapeutics for targeting this class of [2Fe-2S] proteins, as well as de novo design of new metalloproteins (44, 45).

Methods

Protein Expression and Purification. Overexpression and purification of the soluble fragment of mitoNEET (amino acids 33–108) and L2 mutants were performed as outlined previously (13). Purification of apo-ferredoxin was performed as outlined previously (46).

Cluster Transfer Kinetics, Potentiometric Redox Titrations, and Cluster Stability Measurements. All UV-visible absorption spectra were measured from the near UV to the near IR (300–800 nm) on a Cary50 spectrophotometer (Varian) equipped with a temperature-controlled cell.

Cluster transfer experiments were performed similarly to previous reports (13). Cluster transfer experiments were performed aerobically at 37 °C at pH 8.0 using 100 μM mitoNEET or L2 mutants and 100 μM apo-ferredoxin in 50 mM Bis-Tris and 100 mM NaCl. The samples were covered with mineral oil (Hampton Research) to prevent losses caused by evaporation. Transfer rates were obtained by following the 423 nm/458 nm ratio corresponding to loss of the mitoNEET 458-nm peak and emergence of the holo-ferredoxin 423-nm peak with time as described previously (13). Data were fit to a single exponential rise, and initial transfer rates were determined by taking the slope of the exponential fit after the first 15 min.

Optical potentiometric redox titrations were performed as outlined previously (32). Briefly, experiments were performed anaerobically at 25 °C under an argon atmosphere using 50 μM mitoNEET or L2 mutants in 100 mM Bis-Tris and 100 mM NaCl in the presence of mediators to facilitate efficient electron transfer between the protein and Ag/AgCl reference electrode (Microelectrodes). Sodium dithionite (Sigma-Aldrich) was titrated in via syringe to reduce the [2Fe-2S] clusters. After mitoNEET was fully reduced, the protein was reoxidized by titrating in 10 μL of fixed aliquots of ambient oxygen. Optical scans (300–800 nm) were performed following each addition of dithionite or oxygen. Optical potentiometric redox titration data were fit to the Nernst equation as described previously (32).

Cluster stability measurements were performed aerobically at 37 °C. Cluster loss was measured over time as a decrease in absorbance at 458 nm. Studies were performed using varying concentrations of mitoNEET and mutants in 100 mM Bis-Tris and 100 mM NaCl at pH 7.0.

Details on crystallization, X-ray data collection, and refinement are provided in *SI Text* and Table S2. The atomic coordinates of the L2 mutants have been deposited in the Protein Data Bank. The A68 insert was deposited under PDB ID code 4EZF, the M62G was deposited under PDB ID code 4F28, the G66A/D67A mutant was deposited under PDB ID code 4F2C, and the D67G mutant was deposited under PDB ID code 4F1E.

All-Atom Simulations. The structure-based models in Gromacs (SMOG) Web tool (http://smog-server.org) (47) was used to generate an all-atom structure-based force field from the crystal structure of mitoNEET stored in PDB ID code 2QH7 (9). The shadow algorithm was used to identify native contacts (48). Simulations were performed using version 4.0.5 of the Groningen Machine for Chemical Simulations (GROMACS) software package (49). The integrator used was stochastic dynamics. The time step τ was 0.0005. Each protomer was temperature coupled separately.

ACKNOWLEDGMENTS. This work was supported in part by the Center for Theoretical Biological Physics sponsored by National Science Foundation (NSF) Grants PHY-0822283 and MCB-1214457 and by National Institutes of Health Grants GM-54038 and GM101467. R.N. acknowledges the support of Israel Science Foundation Grant 863/09, and E.L.B. was also supported by a San Diego Fellowship. J.A.Z. was supported by Heme and Blood Proteins Training Grant GN 5T32DK007233-34. J.N.O. is a CPRIT Scholar in Cancer Research sponsored by the Cancer Prevention and Research Institute of Texas (CPRIT). H.L.A. acknowledges the support of the National Institute of General Medical Sciences Protein Structure Initiative (U54GM094586) at the Joint Center for Structural Genomics. Portions of this research were carried out at the Stanford Synchrotron Radiation Lightsource (SSRL), a Directorate of the SLAC National Accelerator Laboratory and an Office of Science User Facility operated for the US Department of Energy (DOE) Office of Science by Stanford University. The SSRL Structural Molecular Biology Program is supported by the DOE Office of Biological and Environmental Research, and by the National Institutes of Health, National Institute of General Medical

Sciences (including P41GM103393) and the National Center for Research Resources (P41RR001209). The contents of this publication are solely the responsibility of the authors and do not necessarily represent the official views of NIGMS, NCRR, or NIH.

1. Beinert H (2000) Iron-sulfur proteins: Ancient structures, still full of surprises. *J Biol Inorganic Chem* 5(1):2–15.
2. Waldron KJ, Rutherford JC, Ford D, Robinson NJ (2009) Metalloproteins and metal sensing. *Nature* 460(7257):823–830.
3. Rees DC, Howard JB (2003) The interface between the biological and inorganic worlds: Iron-sulfur metalloclusters. *Science* 300(5621):929–931.
4. Gray HB, Winkler JR (1996) Electron transfer in proteins. *Annu Rev Biochem* 65: 537–561.
5. Bertini I (2007) *Biological Inorganic Chemistry: Structure and Reactivity* (University Science Books, Sausalito, CA), p xxv.
6. Napier I, Ponka P, Richardson DR (2005) Iron trafficking in the mitochondrion: novel pathways revealed by disease. *Blood* 105(5):1867–1874.
7. Johnson DC, Dean DR, Smith AD, Johnson MK (2005) Structure, function, and formation of biological iron-sulfur clusters. *Annu Rev Biochem* 74:247–281.
8. Lill R, Mühlenhoff U (2008) Maturation of iron-sulfur proteins in eukaryotes: mechanisms, connected processes, and diseases. *Annu Rev Biochem* 77:669–700.
9. Paddock ML, et al. (2007) MitoNEET is a uniquely folded 2Fe 2S outer mitochondrial membrane protein stabilized by pioglitazone. *Proc Natl Acad Sci USA* 104(36): 14342–14347.
10. Hou X, et al. (2007) Crystallographic studies of human MitoNEET. *J Biol Chem* 282(46): 33242–33246.
11. Lin J, Zhou T, Ye K, Wang J (2007) Crystal structure of human mitoNEET reveals distinct groups of iron sulfur proteins. *Proc Natl Acad Sci USA* 104(37):14640–14645.
12. Conlan AR, et al. (2011) Mutation of the His ligand in mitoNEET stabilizes the 2Fe-2S cluster despite conformational heterogeneity in the ligand environment. *Acta Crystallogr D Biol Crystallogr* 67(Pt 6):516–523.
13. Zuris JA, et al. (2011) Facile transfer of [2Fe-2S] clusters from the diabetes drug target mitoNEET to an apo-acceptor protein. *Proc Natl Acad Sci USA* 108(32):13047–13052.
14. Bak DW, Zuris JA, Paddock ML, Jennings PA, Elliott SJ (2009) Redox characterization of the FeS protein MitoNEET and impact of thiazolidinedione drug binding. *Biochemistry* 48(43):10193–10195.
15. Colca JR, et al. (2004) Identification of a novel mitochondrial protein ("mitoNEET") cross-linked specifically by a thiazolidinedione photoprobe. *Am J Physiol Endocrinol Metab* 286(2):E252–E260.
16. Hernández C, Genescà J, Ignasi Esteban J, García L, Simó R (2000) Relationship between iron stores and diabetes mellitus in patients infected by hepatitis C virus: A case-control study. *Med Clin (Barc)* 115(1):21–22.
17. Jiang R, et al. (2004) Body iron stores in relation to risk of type 2 diabetes in apparently healthy women. *JAMA* 291(6):711–717.
18. Baxter EL, Jennings PA, Onuchic JN (2011) Interdomain communication revealed in the diabetes drug target mitoNEET. *Proc Natl Acad Sci USA* 108(13):5266–5271.
19. Baxter EL, Jennings PA, Onuchic JN (2012) Strand swapping regulates the iron-sulfur cluster in the diabetes drug target mitoNEET. *Proc Natl Acad Sci USA* 109(6): 1955–1960.
20. Leopold PE, Montal M, Onuchic JN (1992) Protein folding funnels: A kinetic approach to the sequence-structure relationship. *Proc Natl Acad Sci USA* 89(18):8721–8725.
21. Bryngelson JD, Onuchic JN, Socci ND, Wolynes PG (1995) Funnels, pathways, and the energy landscape of protein folding: A synthesis. *Proteins* 21(3):167–195.
22. Kalbitzer HR, Spoerner M, Ganser P, Hozsa C, Kremer W (2009) Fundamental link between folding states and functional states of proteins. *J Am Chem Soc* 131(46): 16714–16719.
23. Jäger M, et al. (2006) Structure-function-folding relationship in a WW domain. *Proc Natl Acad Sci USA* 103(28):10648–10653.
24. Karanicolas J, Brooks CL, 3rd (2004) Integrating folding kinetics and protein function: Biphasic kinetics and dual binding specificity in a WW domain. *Proc Natl Acad Sci USA* 101(10):3432–3437.
25. Ferreiro DU, Hegler JA, Komives EA, Wolynes PG (2007) Localizing frustration in native proteins and protein assemblies. *Proc Natl Acad Sci USA* 104(50):19819–19824.
26. Capraro DT, Roy M, Onuchic JN, Jennings PA (2008) Backtracking on the folding landscape of the beta-trefoil protein interleukin-1beta? *Proc Natl Acad Sci USA* 105 (39):14844–14848.
27. Gosavi S, Whitford PC, Jennings PA, Onuchic JN (2008) Extracting function from a beta-trefoil folding motif. *Proc Natl Acad Sci USA* 105(30):10384–10389.
28. Gosavi S, Chavez LL, Jennings PA, Onuchic JN (2006) Topological frustration and the folding of interleukin-1 beta. *J Mol Biol* 357(3):986–996.
29. Clementi C, Nymeyer H, Onuchic JN (2000) Topological and energetic factors: what determines the structural details of the transition state ensemble and "en-route" intermediates for protein folding? An investigation for small globular proteins. *J Mol Biol* 298(5):937–953.
30. Lammert H, Schug A, Onuchic JN (2009) Robustness and generalization of structure-based models for protein folding and function. *Proteins* 77(4):881–891.
31. Whitford PC, et al. (2009) An all-atom structure-based potential for proteins: bridging minimal models with all-atom empirical forcefields. *Proteins* 75(2):430–441.
32. Zuris JA, et al. (2010) Engineering the redox potential over a wide range within a new class of FeS proteins. *J Am Chem Soc* 132(38):13120–13122.
33. Wiley SE, Murphy AN, Ross SA, van der Geer P, Dixon JE (2007) MitoNEET is an iron-containing outer mitochondrial membrane protein that regulates oxidative capacity. *Proc Natl Acad Sci USA* 104(13):5318–5323.
34. Whitford PC, Miyashita O, Levy Y, Onuchic JN (2007) Conformational transitions of adenylate kinase: Switching by cracking. *J Mol Biol* 366(5):1661–1671.
35. Roy M, et al. (2005) The native energy landscape for interleukin-1beta. Modulation of the population ensemble through native-state topology. *J Mol Biol* 348(2):335–347.
36. Haliloglu T, Bahar I (1998) Coarse-grained simulations of conformational dynamics of proteins: application to apomyoglobin. *Proteins* 31(3):271–281.
37. Ratje AH, et al. (2010) Head swivel on the ribosome facilitates translocation by means of intra-subunit tRNA hybrid sites. *Nature* 468(7324):713–716.
38. Whitford PC, et al. (2010) Accommodation of aminoacyl-tRNA into the ribosome involves reversible excursions along multiple pathways. *RNA* 16(6):1196–1204.
39. Chavez LL, Gosavi S, Jennings PA, Onuchic JN (2006) Multiple routes lead to the native state in the energy landscape of the β-trefoil family. *Proc Natl Acad Sci USA* 103(27): 10254–10258.
40. Fan YX, Ju M, Zhou JM, Tsou CL (1995) Activation of chicken liver dihydrofolate reductase in concentrated urea solutions. *Biochim Biophys Acta* 1252(1):151–157.
41. Zhang HJ, Sheng XR, Pan XM, Zhou JM (1997) Activation of adenylate kinase by denaturants is due to the increasing conformational flexibility at its active sites. *Biochem Biophys Res Commun* 238(2):382–386.
42. Duffy TH, Sato JK, Vitols KS, Huennekens FM (1985) L1210 dihydrofolate reductase: Activation and enhancement of methotrexate sensitivity. *Adv Enzyme Regul* 24: 13–25.
43. Nechushtai R, et al. (2011) Allostery in the ferredoxin protein motif does not involve a conformational switch. *Proc Natl Acad Sci USA* 108(6):2240–2245.
44. DeGrado WF, Summa CM, Pavone V, Nastri F, Lombardi A (1999) De novo design and structural characterization of proteins and metalloproteins. *Annu Rev Biochem* 68: 779–819.
45. Lu Y, Yeung N, Sieracki N, Marshall NM (2009) Design of functional metalloproteins. *Nature* 460(7257):855–862.
46. Fish A, Danieli T, Ohad I, Nechushtai R, Livnah O (2005) Structural basis for the thermostability of ferredoxin from the cyanobacterium Mastigocladus laminosus. *J Mol Biol* 350(3):599–608.
47. Noel JK, Whitford PC, Sanbonmatsu KY, Onuchic JN (2010) SMOG@ctbp: Simplified deployment of structure-based models in GROMACS. *Nucleic Acids Res* 38(web server issue):W657–W661.
48. Noel JK, Whitford PC, Onuchic JN (2012) The shadow map: A general contact definition for capturing the dynamics of biomolecular folding and function. *J Phys Chem B* 116(29):8692–8702.
49. Hess B, Kutzner C, van der Spoel D, Lindahl E (2008) GROMACS 4: Algorithms for highly efficient, load-balanced, and scalable molecular simulation. *J Chem Theory Comput* 4(3):435–447.